

Shock-Wave Resistance of WS₂ Nanotubes

Yan Qiu Zhu,[†] Toshimori Sekine,[‡] Kieren S. Brigatti,[†] Steve Firth,[§] Reshef Tenne,^{||}
Rita Rosentsveig,^{||} Harold W. Kroto,[†] and David R. M. Walton^{*,†}

Contribution from the Fullerene Science Centre, School of Chemistry, Physics & Environmental Science, University of Sussex, Brighton BN1 9QJ, U.K., Advanced Materials Laboratory, National Institute for Materials Science, 1-1 Namiki, Tsukuba 305-0044, Japan, Christopher Ingold Laboratories, University College London, 20 Gordon Street, London WC1H 0AJ, U.K., and Department of Materials and Interfaces, Weizmann Institute of Science, Rehovot 76100, Israel

Received September 24, 2002; E-mail: d.walton@sussex.ac.uk

Abstract: The shock-wave resistance of WS₂ nanotubes has been studied and compared to that of carbon nanotubes. Detailed structural features of post-shock samples were investigated using HRTEM, XRD, and Raman spectroscopy. WS₂ nanotubes are capable of withstanding shear stress caused by shock waves of up to 21 GPa, although some nanotube tips and nanoparticles containing multiple structural defects in the bending regions are destroyed. Small WS₂ species, consisting of only a few layers, are extruded from the nanotubes. Well-crystallized tube bodies were found to exhibit significant stability under shock, indicating high tensile strength. XRD and Raman analyses have confirmed this structural stability. Under similar shock conditions, WS₂ tubes are more stable than carbon nanotubes, the latter being transformed into a diamond phase. WS₂ nanotubes containing small concentrations of defects possess significantly higher mechanical strength, and, as a consequence, hollow WS₂ nanoparticles are expected to act as excellent lubricants under much higher loading than was previously thought.

Introduction

Following the discovery of carbon nanotubes in 1991,¹ Tenne and co-workers^{2–4} observed that fullerene-like cage structures and nanotubes could be obtained from laminated MX₂ (M = Mo or W; X = S, Se, or Te) compounds. This work resulted in the formation of novel layered materials which, unlike single-layered graphite¹ and double-layered B–C–N nanotubes,⁵ exhibit multiple-layered closed nanostructures. To date, inorganic fullerene-like structure research has focused primarily on production^{6–9} and the study of wear-resistant properties.^{10–12} As a consequence, various new forms of nanotubes, including

NbS₂,^{13–16} mixed phased,^{17–18} single-layered WS₂,¹⁹ and MoS₂²⁰ nanotubes, have been prepared successfully. Nanotubes and fullerene-like materials were also made from various layered oxides and halides. These MX₂ species resemble carbon nanotubes in that they are generally well-crystallized; however, sometimes the residues from their corresponding oxide will be present in the central hollow cores. Such MX₂ species are extraordinarily wear-resistant when used as solid lubricants,^{10–12} and they can also be employed as nanoscale electron microscope probe tips.²¹ Superior physical properties, as exemplified by superconducting NbS₂, have also been predicted;²² however, direct experimental assessment of the mechanical behavior of these inorganic nanotubes (including nanoparticles) has yet to be described.

Shock waves generate concurrently extremely high dynamic pressures and temperatures.²³ Pressure propagation in samples causes very high shear stresses, within 1 μs, thereby differing

[†] University of Sussex.

[‡] National Institute for Materials Science.

[§] University College London.

^{||} Weizmann Institute of Science.

- (1) Iijima, S. *Nature* **1991**, *354*, 56.
- (2) Tenne, R.; Margulis, L.; Genut, M.; Hodes, G. *Nature* **1992**, *360*, 444.
- (3) Margulis, L.; Salltra, G.; Tenne, R.; Talianker, M. *Nature* **1993**, *365*, 144.
- (4) Tsirlina, T.; Feldman, Y.; Homyonfer, M.; Sloan, J.; Hutchison, J. L.; Tenne, R. *Fullerene Sci. Technol.* **1998**, *6*, 157.
- (5) Stephan, O.; Ajayan, P. M.; Colliex, C.; Redlich, P.; Lambert, J. M.; Bernier, P.; Lefin, P. *Science* **1994**, *266*, 1683.
- (6) Remskar, M.; Skraba, Z.; Ballif, C.; Sanjines, R.; Levy, F. *Surf. Sci.* **1999**, *433–435*, 637.
- (7) Rothschild, A.; Frey, G. L.; Homyonfer, M.; Tenne, R.; Rappaport, M. *Mater. Res. Innovations* **1999**, *3*, 145.
- (8) Zhu, Y. Q.; Hsu, W. K.; Grobert, N.; Chang, B. H.; Terrones, M.; Terrones, H.; Kroto, H.; Walton, D. R. M. *Chem. Mater.* **2000**, *12*, 1190.
- (9) Rosentsveig, R.; Margolin, A.; Feldman, Y.; Popovitz-Biro, R.; Tenne, R. *Appl. Phys. A* **2002**, *74*, 367.
- (10) Rapoport, L.; Bilik, Y.; Feldman, Y.; Homyonfer, M.; Cohen, S. R.; Tenne, R. *Nature* **1999**, *387*, 791.
- (11) Rapoport, L.; Feldman, Y.; Homyonfer, M.; Cohen, H.; Sloan, J.; Hutchison, J. L.; Tenne, R. *Wear* **1999**, *229*, 975.
- (12) Chhowalla, M.; Amaratunga, G. A. J. *Nature* **2000**, *407*, 164.

- (13) Remskar, M.; Mrzel, A.; Jesih, A.; Levy, F. *Adv. Mater.* **2002**, *14*, 680.
- (14) Schuffenhauer, C.; Popovitz-Biro, R.; Tenne, R. *J. Mater. Chem.* **2002**, *12*, 1587.
- (15) Zhu, Y. Q.; Hsu, W. K.; Kroto, H. W.; Walton, D. R. M. *Chem. Commun.* **2001**, *21*, 2184.
- (16) Nath, M.; Rao, C. N. R. *J. Am. Chem. Soc.* **2001**, *123*, 4841.
- (17) Hsu, W. K.; Zhu, Y. Q.; Yao, N.; Firth, S.; Clark, R. J. H.; Kroto, H. W.; Walton, D. R. M. *Adv. Funct. Mater.* **2001**, *1*, 69.
- (18) Zhu, Y. Q.; Hsu, W. K.; Terrones, M.; Firth, S.; Grobert, N.; Clark, R. J. H.; Kroto, H. W.; Walton, D. R. M. *Chem. Commun.* **2001**, *1*, 121.
- (19) Remskar, M.; Mrzel, A.; Skraba, Z.; Jesih, A.; Ceh, M.; Demsar, J.; Stadelmann, P.; Levy, F.; Mihailovic, D. *Science* **2001**, *292*, 479.
- (20) Whitby, R. L. D.; Hsu, W. K.; Boothroyd, C. B.; Fearon, P. K.; Kroto, H. W.; Walton, D. R. M. *ChemPhysChem* **2001**, *10*, 620.
- (21) Rothschild, A.; Cohen, S. R.; Tenne, R. *Appl. Phys. Lett.* **1999**, *75*, 4025.
- (22) Seifert, G.; Terrones, H.; Terrones, M.; Frauenheim, T. *Solid State Commun.* **2000**, *115*, 635.

from stresses produced by static pressure.²³ A systematic investigation of the microstructure and phase transformation of post-shock samples provides valuable information concerning mechanical and other properties, particularly in the context of applications. Using a single stage powder gun,²⁴ we previously studied phase changes and structural features of multiwalled carbon nanotubes.²⁵ Severe structural damage occurred, and a new diamond phase was detected in the post-shock sample (pressure > 20 GPa). In this paper, we report that multiwalled WS₂ nanotubes exhibit superior mechanical properties, surviving shear stresses at high pressures (>20 GPa) induced by shock waves. Detailed structural studies of post-shock samples have revealed that no phase changes take place and that most of the nanotubes are well-preserved. Thus, it appears that inorganic nanotubes can survive much more intense shocks than can carbon nanotubes.

Experimental Section

WS₂ nanotube powder (ca. 100 mg) was sandwiched between two copper disks (12 mm in diameter, 2 mm thick) and pressed into a stainless steel sample holder which was placed in a steel container to protect the contents from destructive shock waves. Two shots were carried out using steel flyers (29 mm diameter, 4 mm thick), at impact velocities of 1.0 and 1.6 km/s, generating 21 and 36 GPa peak pressures, respectively, based on the impedance match method. The detailed experimental setup and method for calculating pressure have been described previously.²⁴ After the impact experiments, the containers were opened, and the samples were removed and subjected to HRTEM, XRD, and Raman analyses. No color change was observed in the dark gray WS₂ samples, after shock compression.

Results and Discussion

Well-Preserved Nanotubes. HRTEM examination of the post-shock samples revealed that some of the WS₂ nanotubes were strong enough to withstand a pressure of 21 GPa. Some of the post-shock nanotubes (Figure 1a) were identical to the pristine samples (Figure 1b): long, straight, and with open tips. The tips (e.g., Figure 1a) do not appear to have been broken by the shock; indeed they clearly resemble the original open-tipped WS₂ nanotube structure produced by the continuous growth process (Figure 1b).⁸ The layer fringe separations are 0.62 nm, that is, the same as those found for normal WS₂ nanotube layer separation.¹ Defects, for example, layer mismatches,²⁶ are also present (Figure 1a, arrow); however, it seems that such defects do not lead to degradation of mechanical properties at this pressure, and the structures are fairly well-preserved.

We found that the nanotubes are more resistant to shear stresses than are the hollow (fullerene-like) WS₂ nanoparticles. A typical nanoparticle suffers severe shock-wave damage (Figure 2a). In particular, deformation and destruction occur in the structurally defective domains, where high stresses are generally located, and three- or four-membered rings may be involved.^{26,27} The inner layers of this particle are still visible;

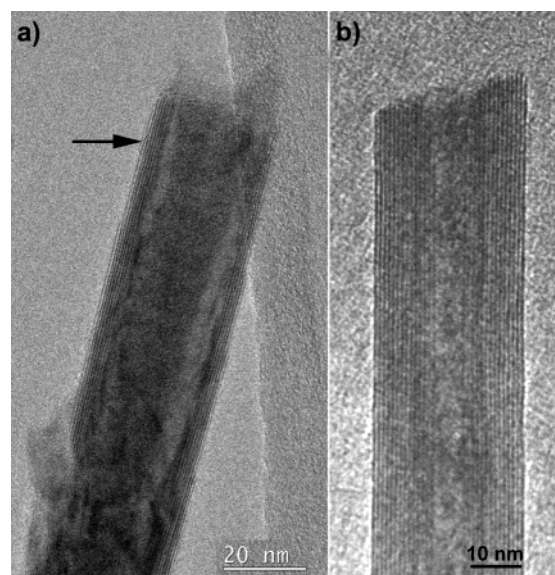


Figure 1. HRTEM images of WS₂ nanotubes with 0.62 nm layer separation: (a) post-shock sample, layer-mismatch arrowed; (b) prior to shock waves.

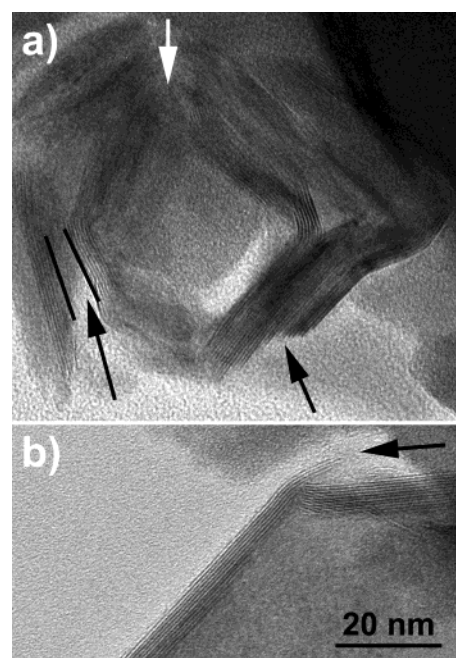


Figure 2. HRTEM images of damaged nanoparticles: (a) broken layers appear at defective sites (black and white arrows); layer relocation has occurred (solid lines) after breakage; (b) broken layers at the junction (arrowed).

however, some of the outer shells are evidently broken (arrowed), and several adjacent layers have become relocated as a result. Nevertheless, the remaining layers exhibit the normal 0.62 nm fringe separation. In the particle shown (Figure 2b), significantly less structural damage is seen, possibly because of its larger size and better crystalline structure. The broken outer layers (Figure 2a) have shifted apparently along the remaining inner onion structure, due to the weak van der Waals interactions between the WS₂ layers. Under such high pressure shock waves, the resulting shear stresses within the particles are likely to be more severe than those encountered by a solid lubricant during a dynamic wearing process. Thus, these inorganic nanoparticles are expected to exhibit lubricating

(23) Horie, Y.; Sawaoka, A. *Compression Chemistry of Materials*; KTK Scientific Publ.: Tokyo, 1993.

(24) Sekine, T. *Eur. J. Solid State Inorg. Chem.* **1997**, *34*, 823.

(25) Zhu, Y. Q.; Sekine, T.; Kobayashi, T.; Takazawa, E.; Terrones, M.; Terrones, H. *Chem. Phys. Lett.* **1998**, *287*, 689.

(26) Zhu, Y. Q.; Hsu, W. K.; Terrones, H.; Grobert, N.; Chang, B. H.; Terrones, M.; Wei, B. Q.; Kroto, H. W.; Walton, D. R. M.; Boothroyd, C. B.; Kinloch, I.; Chen, G. Z.; Windle, A. H.; Fray, D. J. *J. Mater. Chem.* **2000**, *10*, 2570.

(27) Sloan, J.; Hutchison, J. L.; Tenne, R.; Feldman, Y.; Tsirlina, T.; Homyonfer, M. *J. Solid State Chem.* **1999**, *144*, 100.

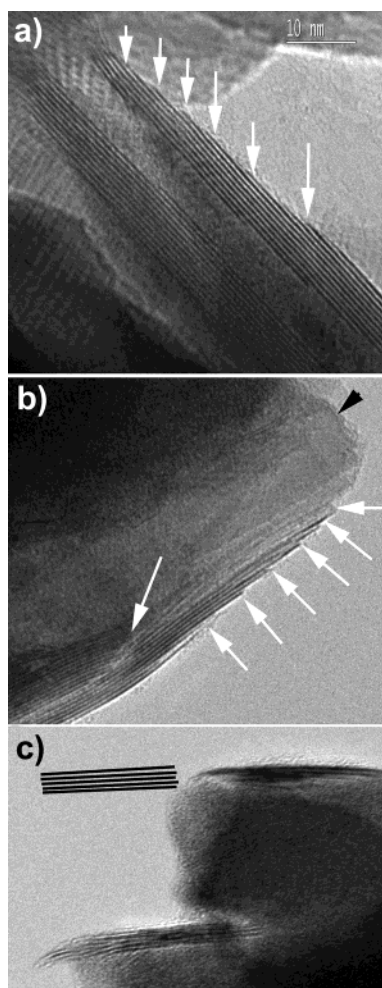


Figure 3. HRTEM images revealing tube tip damage: (a) the tip cap has been removed, and a needlelike feature is seen on one side of the tube wall (arrowed); (b) the tip cap has also been removed, and a needlelike wall feature and layer deformation are apparent; a two-layered tip cap residue is indicated by the black arrow; (c) part of the tube body has been removed together with its tip; solid lines represent the removed tube walls.

properties and to be applicable at higher and more severe loading stresses than most currently used lubricants can withstand (<1 GPa).

WS₂ Structural Damage. Structural damage has been assessed in detail by HRTEM, particularly at the tube tip. Several types of tip deformation are shown in Figure 3. In Figure 3a, originally an ca. 10-layered nanotube, the tip is open, and some of its outer layers have been removed. Severe damage is apparent closer to the tip, especially on the right-hand side of the wall (arrowed). This needlelike feature is also shown in Figure 3b, the outer layers toward the end of the tube having been removed progressively (white arrows). However, the residue of a two-layered cap partly wrapping this tip (black arrow) is apparent, possibly because the inner WO_x core mechanically supports the tube. The most significant damage to these nanotubes is indicated by partial exfoliation of the tube walls (Figure 3c). One-half of the walls, including the inner oxide core, have been destroyed to the extent that the tube shape is hardly recognizable (solid lines represent missing tube walls). The role that the central WO_x cores play in the context of the presence of shock-wave pressure is likely to be complex. First, such cores would mechanically support the outer tube shells during the passage of the shock wave, as indicated by Figure

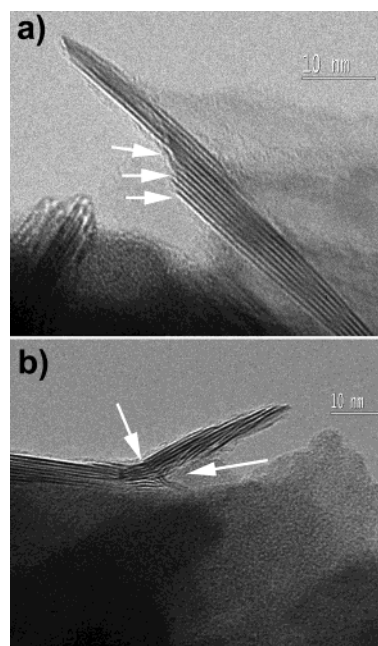


Figure 4. HRTEM images of WS₂ species: (a) from a tube body, the broken site and its needlelike feature are arrowed (white); (b) being removed from a tube body, arrows pointing to the deformation sites.

3b. This supporting effect seems to be dominant, while the local pressure resembles a standard static pressure. Second, the structure of the oxide cores differs from the outer WS₂ layer. The oxide crystals are more rigid and lack flexibility under stress, whereas the layered WS₂ can behave as a spring absorbing the shock pressure. In cases where the local pressures are more dynamic, the central oxide core might initiate breakage of the whole nanotube, a negative effect thus being observed (Figure 3c).

Although open-tipped WS₂ tubes are often observed prior to shock-wave treatment, we believe that some of the open-tipped structures arise from the shock waves and are caused by associated shear stress. Such damaged tip features are consistent with the fact that the nanoparticles are severely deformed during shock treatment, because of the high concentration of defects originally present in the tips. The fact that hollow nanoparticles (Figure 2) suffer relatively greater shock damage than do nanotubes can be attributed to the larger stresses and strains in the former. Nanotubes, in which layers are folded only along one axis, are less strained and chemically more stable than the nested fullerene-like nanoparticles of WS₂. Thus, structurally high quality nanotubes (containing fewer defects), as shown in Figure 1a, appear to be able to survive much higher shock-wave pressures and shear stresses. More spherical hollow nanoparticles containing fewer corners, and thus fewer defects, would be expected to exhibit higher pressure resistance.

Another kind of tube tip damage is shown in Figure 4. Minute WS₂ flakes, consisting of 2–10 layers (Figure 4a), have separated or have nearly peeled from the tube body (Figure 4b). The layer front (Figure 4a, arrowed) exhibits a progressively broken feature, corresponding to the body of a nanotube. The severe deformation, arrowed in Figure 4b, clearly showed how the actual shear stresses led to destruction of the tubes, and how the flakes were removed from a tube or a particle, leading to deformed structures. The initial structural defects correspond apparently to the sites where deformations started. It is

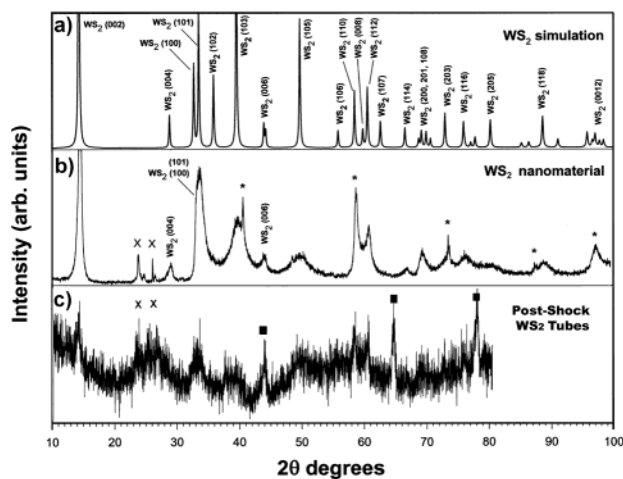


Figure 5. XRD profiles: (a) simulation from WS₂ nanocrystals; (b) WS₂ nanotubes prior to shock waves, in which peaks marked “x” are due to WO_x, and those marked “*” are due to the W residue; (c) post-shock WS₂ tubes; solid squares represent β -W peaks.

noteworthy that survival of the tiny WS₂ flakes (Figure 4) and the relatively thinner whole nanotube (Figure 1a) appears to indicate that the smaller the size (diameter or less number of layers) of the species, the higher the resistance to the shock waves. The larger particles are more likely to be damaged (Figure 2).

XRD and Raman Analyses. Post-shock samples were subjected to X-ray powder diffraction analysis (Cu K α radiation; scanning rate 0.02 deg/min), to characterize any overall structural change. By comparison with the XRD profiles of the simulated hexagonal WS₂ nanocrystal (Figure 5a) and the WS₂ nanotubes prior to shock treatment (Figure 5b),²⁶ we found that significant structural changes had occurred in the post-shock samples (Figure 5c), as indicated by a significant weakening (002) intensity (Figure 5c). However, we observed no shift in the position of the (002) peak of WS₂, indicating that the 0.62 nm layer separation remains unchanged, even for damaged species, consistent with HRTEM investigations. The WHPH (width of half peak height) of the (002) peak has increased considerably, because of the average smaller size of the crystalline domains which remain post shock. Many damaged structures, as observed by HRTEM, contain fewer layers after the shock. The higher angle peaks (except 004 which appears to be rather weak) seem to be relatively stronger and still remain in the same positions. We believe that the shock-induced shear stresses do not produce any significant effect on the inner layer structures. The loss of original intensity is indicative of the loss of crystallinity of the sample. However, the fact that these peaks are still present shows that the basic structure is unchanged. Furthermore, the hollow tube and onion nanostructures are likely to absorb most of the shock energy. The WO_x phases, marked by “x” in the XRD profiles (Figure 5b and c), are present in both the pristine and the post-shock nanotube samples. However, the W residue, present in the original sample and identified by “*” in Figure 5b, has disappeared after shock. The three strong peaks, at 44, 65, and 78 2 θ degrees, marked by black squares, have appeared. Considering the copper disks used in the shock sample assembly, we find that it is likely that they reacted with the tungsten due to the high temperatures generated during the shock. However, such a resulting W–Cu alloy would not significantly affect the 2 θ value. These peaks are assigned to

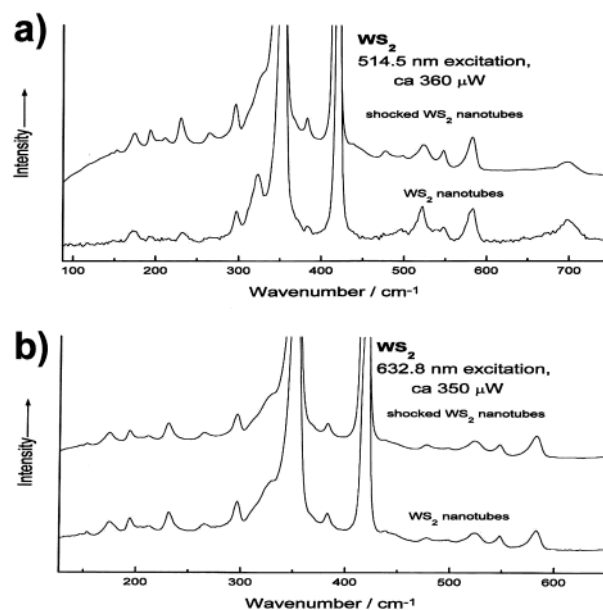


Figure 6. WS₂ nanotube Raman spectra: (a) before and after shock at 514.5 nm excitation; (b) before and after shock at 632.8 nm excitation.

the (211), (222), and (400) of β -W (PDF 47-1319), which are transformed from the original W (PDF 4-806) residue during the shock.²⁶

Raman spectra of the WS₂ nanotubes were recorded using 514.5 and 632.8 nm excitation wavelengths. The spectra of the pre- and post-shock samples are almost identical, except that the 323 cm⁻¹ band in the 514.5 nm excitation spectrum of unshocked WS₂ tubes broadens to a shoulder in the spectrum of the shocked tubes (Figure 6a). However, this band also appears as a shoulder in the spectrum of both samples excited with 632.8 nm radiation, so this is not a significant change. It should be noted that the 153 cm⁻¹ band, with 632.8 nm excitation, is present in the spectra of both post- and pre-shocked tubes. This band has been assigned to a disorder-induced Brillouin zone edge phonon that occurs in the spectra of WS₂ nanotubes and particles, but not in the spectrum of bulk hexagonal WS₂.²⁸ The presence of this band in the post-shocked WS₂ nanotube spectrum indicates that little structural change occurred during the shock.

The overall XRD and Raman studies reveal that the majority of inorganic WS₂ nanostructures are strong enough to withstand 21 GPa shock waves. As compared to carbon nanotubes, in which a diamond phase is formed at similar pressures, we find that the inorganic tubes appear to be significantly more stable. They are also more stable than the W residue in the sample, of which a phase transformation to β -W has been observed. A further increase in shock pressures up to 35.6 GPa, achieved by increasing shot pellet speeds to 1.6 km/s, results in severe destruction of the WS₂ nanostructures. No tubular structures were found during the HRTEM examination; however, a deformed nanofiber was observed (Figure 7). We believe that this fiber must have arisen from a WS₂ nanotube damaged during the shock process.

The chemical composition of the post-shock samples was also studied by EDX. The results reveal that after shock treatment

(28) Frey, G. L.; Tenne, R.; Matthews, M. J.; Dresselhaus, M. S.; Dresselhaus, G. *J. Mater. Res.* **1998**, *13*, 2412.

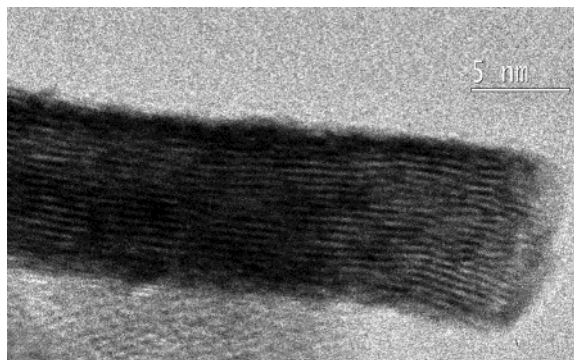


Figure 7. HRTEM image of a WS₂ nanofiber, arising from a nanotube submitted to 35.6 GPa shock waves.

at 21 GPa, the nanotubes consist of an ca. 1:2 W:S ratio, which means that no composition change has taken place; however, minute amounts of O are present in the samples shocked at 35.6 GPa, possibly because the high temperatures result in nanotube oxidation. Such oxidations occur at the outer shells of a

nanotube, as it differs from the oxides remaining after incomplete sulfidation of the nanotubes in the central core.

Conclusions

Inorganic WS₂ nanotubes are capable of withstanding severe shear stress associated with 21 GPa shock waves. Some of the tips and nanoparticles, which contain significant structural defects located at the bending domains, are destroyed. Very small WS₂ species, consisting of only a few layers, are found in the sample. The well-crystallized tube bodies exhibit significant degrees of stability. XRD and Raman analyses have revealed that no phase transformations occur during the shock process. These results indicate that nanotubes containing low concentrations of defects possess high mechanical stability. The nanotubes are destroyed by 35 GPa shock waves.

Acknowledgment. The authors thank the EPSRC for financial support.

JA021208I